Electronic Supplementary Material (ESI) for Faraday Discussions.

Supplementary Information

Facile assembly of layer-interlocked graphene heterostructures as flexible electrodes for Li-ion batteries

Gang Wang, Guangbo Chen, Sheng Yang, Panpan Zhang, Faxing Wang, Ali Shaygan Nia, Minghao Yu and Xinliang Feng*

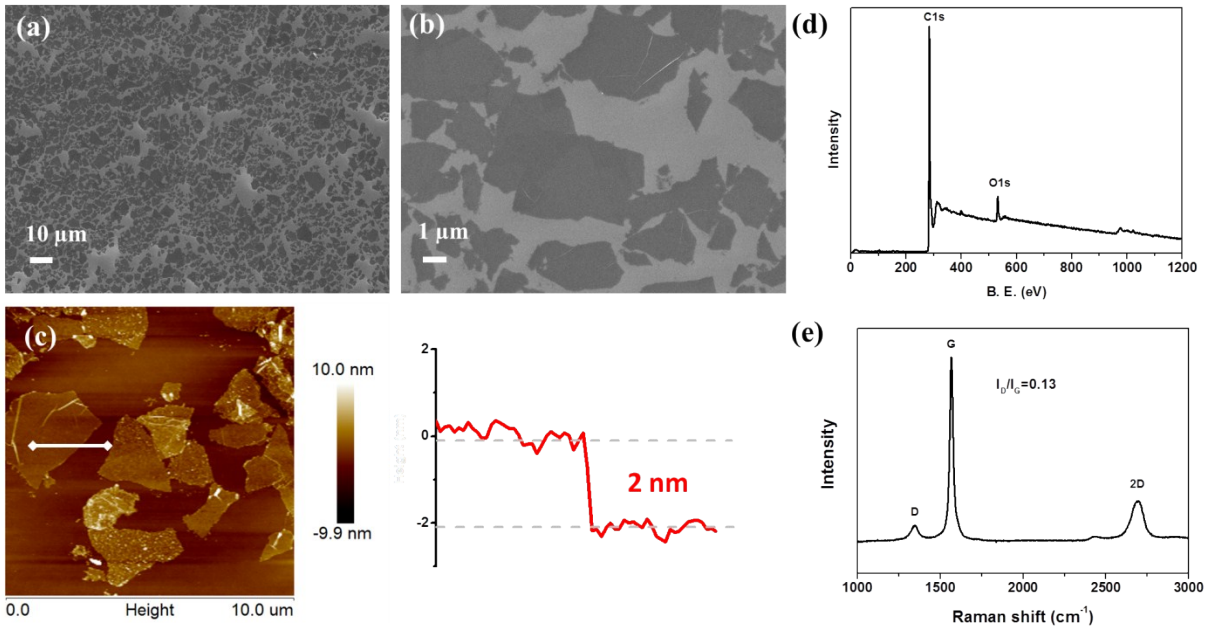

Figure S1. Characterization of EG. SEM (a, b) and AFM (c) images of EG. (d) X-ray photoelectron spectroscopy (XPS) and (e) Raman spectroscopy of EG.

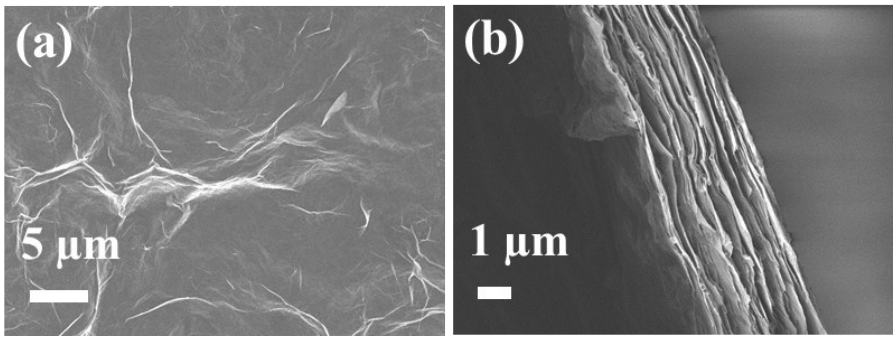

Figure S2. Top-view and edge-view SEM images of EG film.

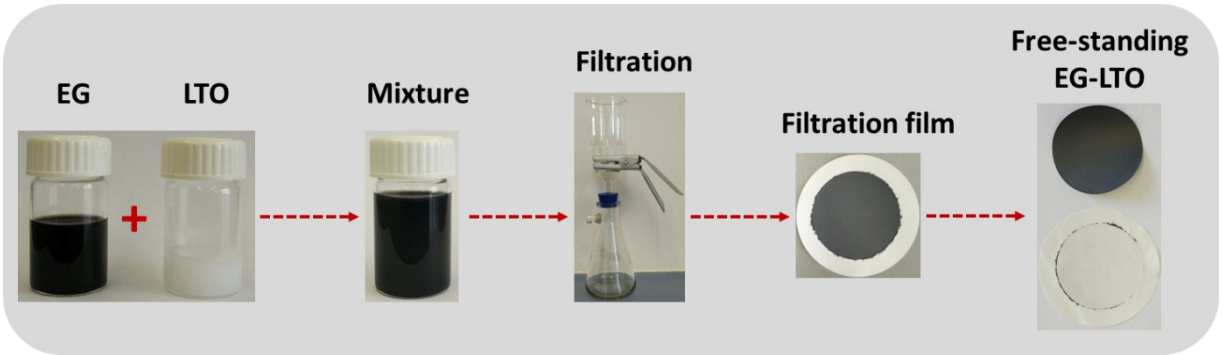

Figure S3. Detailed fabrication procedures of EG-LTO hybrids.

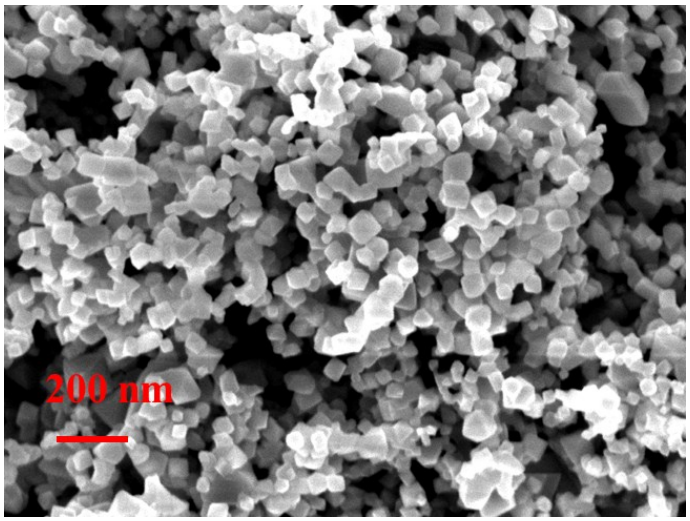

Figure S4. SEM image of spinel LTO NPs.

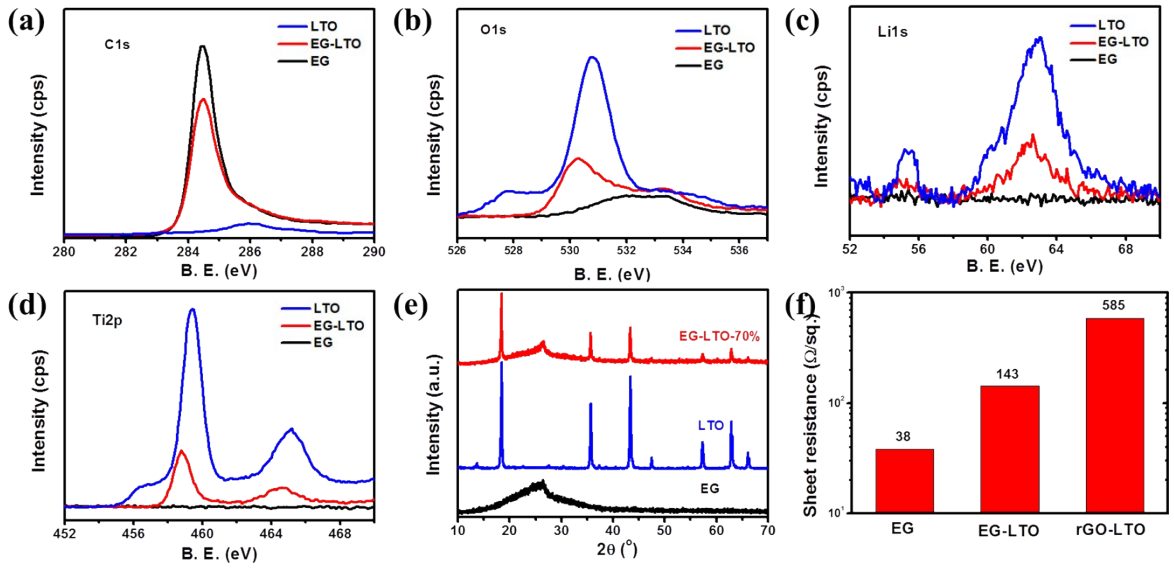

Figure S5. High-resolution X-ray photoelectron C1s, O1s, Li1s and Ti2p spectra (a-d) and XRD patterns (e) of EG, LTO and EG-LTO. (f) Sheet resistance of EG, EG-LTO and rGO-LTO hybrid films measured by a four-point probe system. The graphene mass in these three samples are similar. LTO content in EG-LTO and rGO-LTO is ~70%.

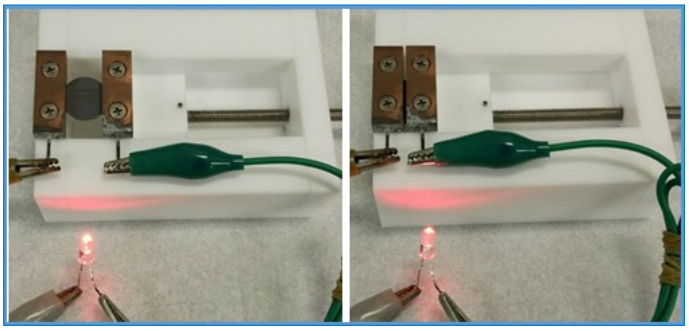

Figure S6. EG paper connected a circuit at different bending states.

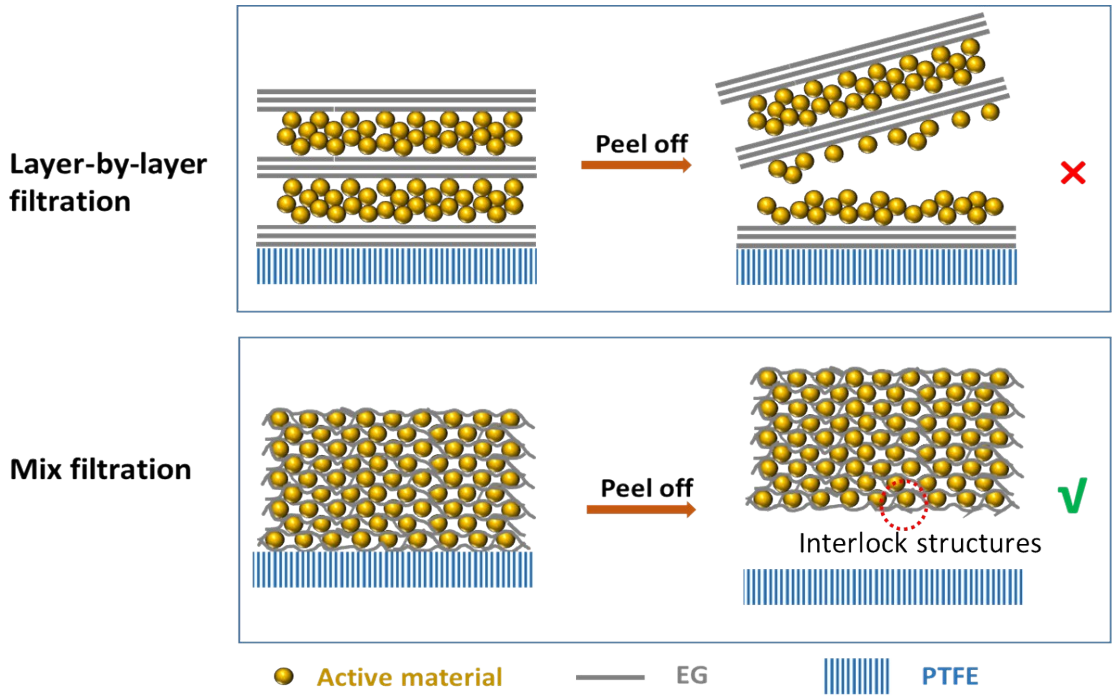

Figure S7. Two different approaches to prepare EG hybrid films, layer-by-layer filtration and mix filtration. Thanks to the presence of interlock structure, EG hybrids from mix filtration exhibited higher mechanical properties than those from layer-by-layer filtration.

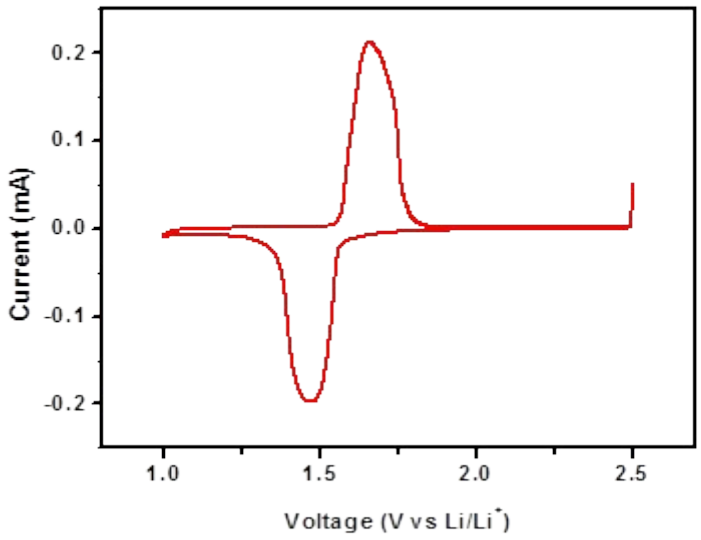

Figure S8. Typical CV curve of EG-LTO hybrid film at a scan rate of 1 mV/s.

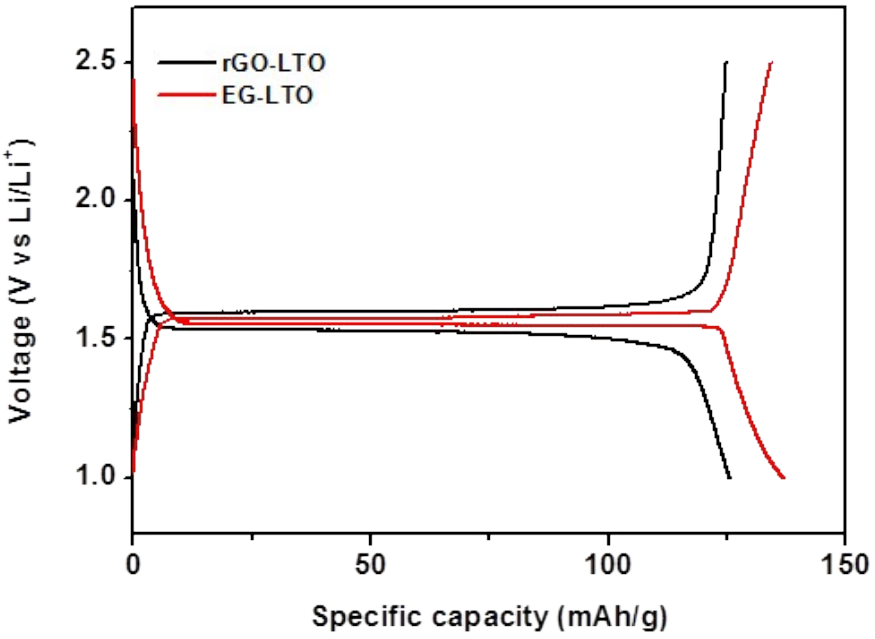

Figure S9. Charge-discharge curves of rGO-LTO and EG-LTO hybrid films at 0.15C.

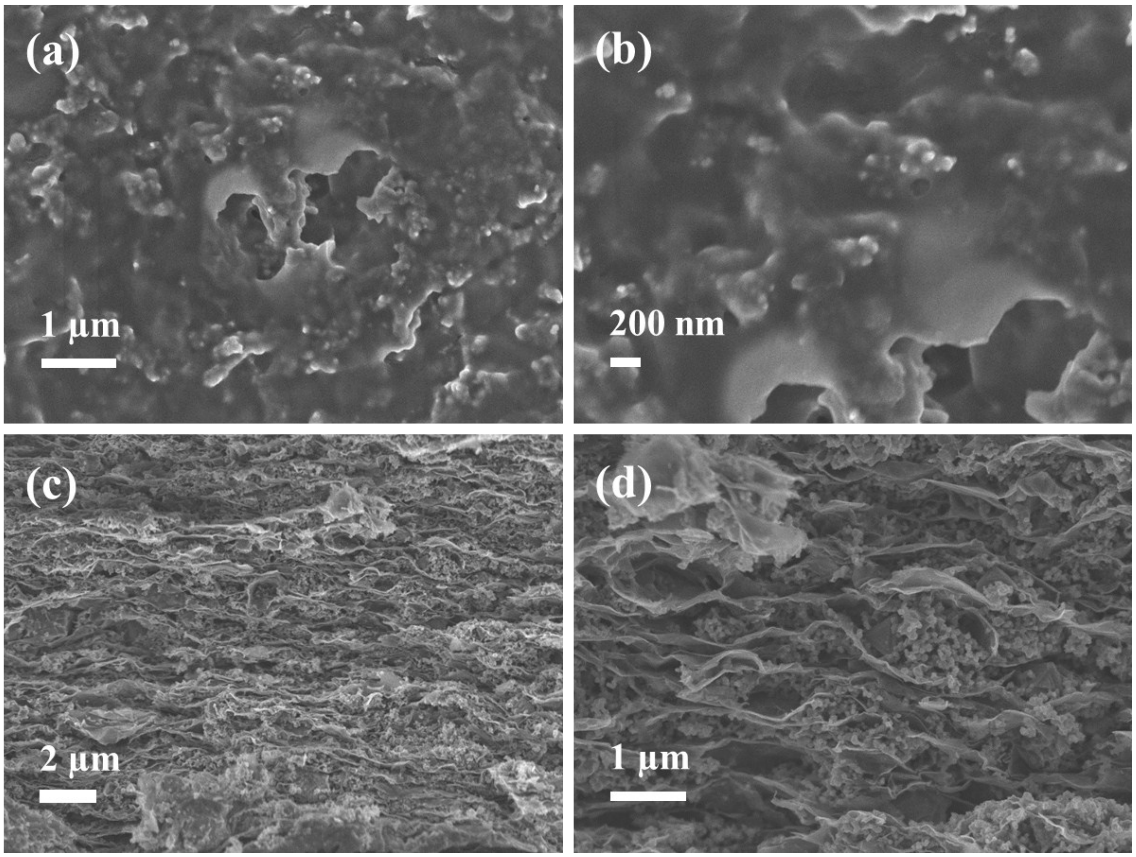

Figure S10. SEM images of EG-LTO hybrid film at 1C for 100 cycles. (a, b) top view, (c, d) edge view.

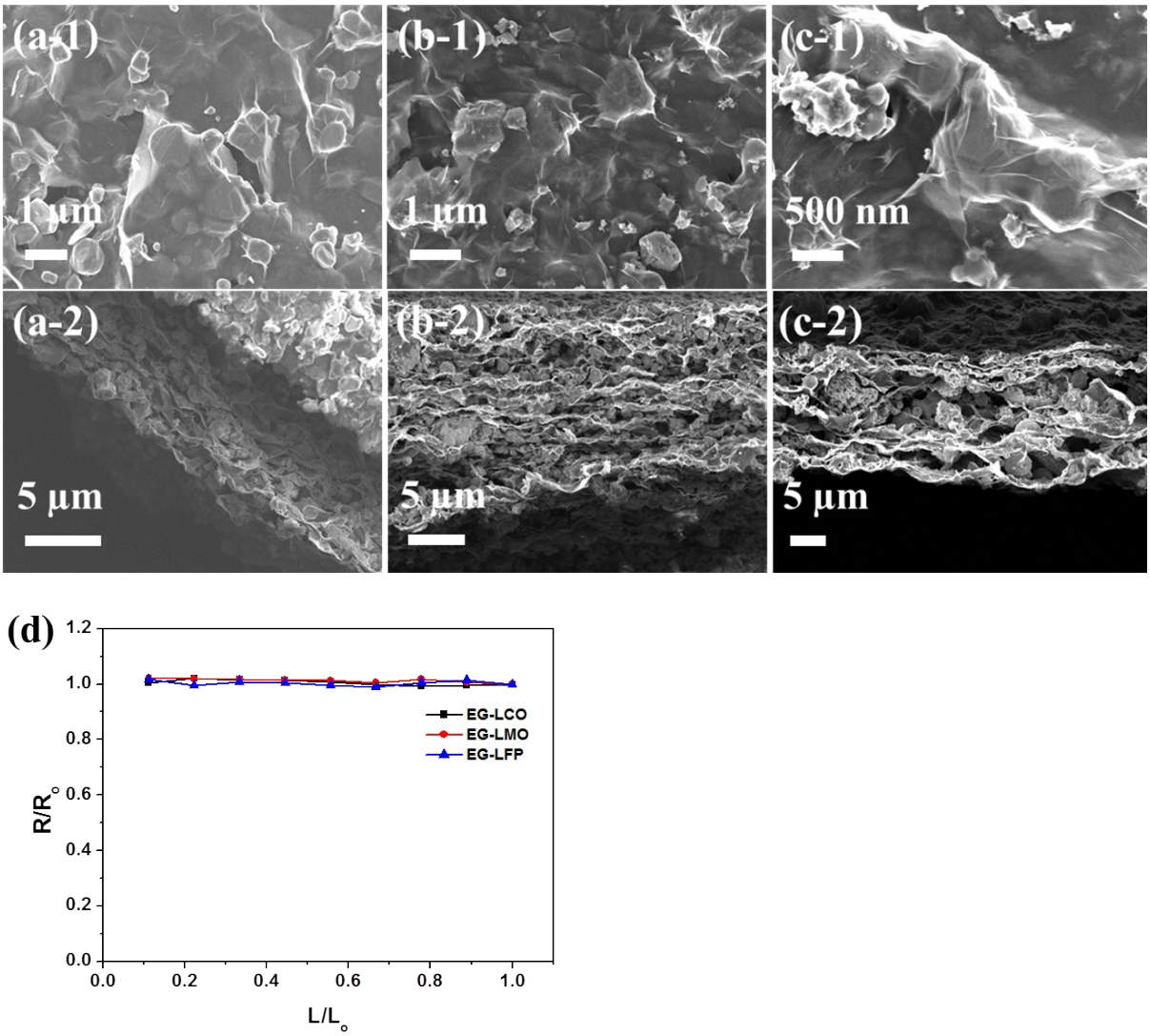

Figure S11. (a-c) SEM images of EG-LCO, EG-LMO and EG-LFP hydrids. (d) Resistance variation of EG-LCO, EG-LMO and EG-LFP hybrids under different bending states.

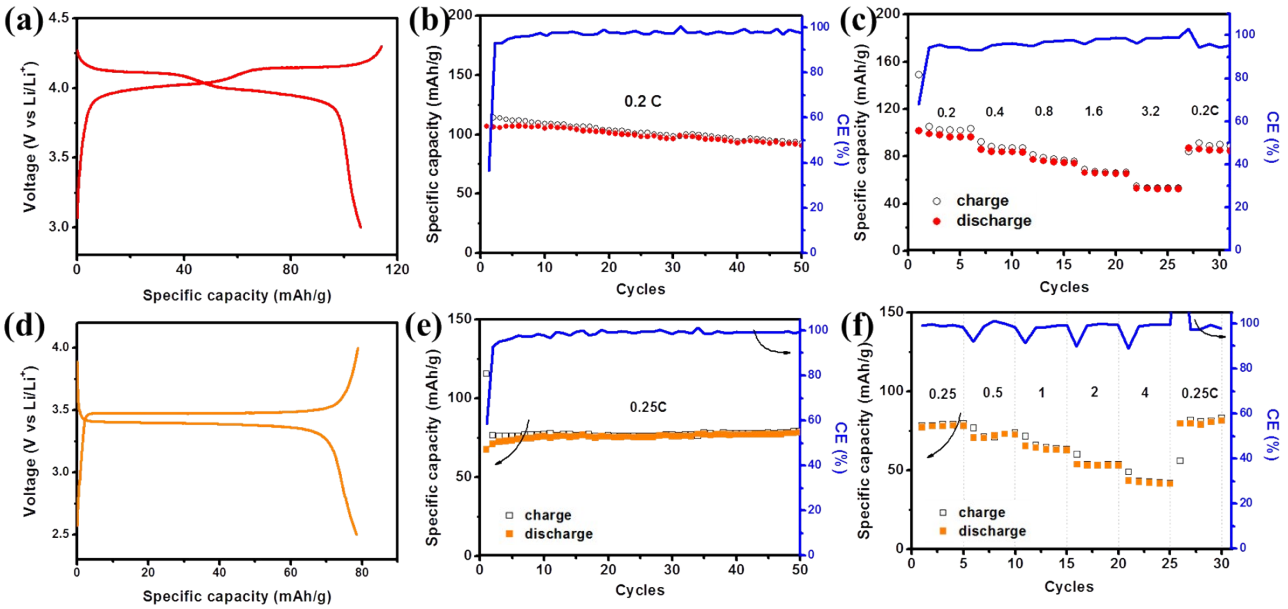

Figure S12. Electrochemical performance of EG-LMO and EG-LFP. (a-c) Charge-discharge curve, cycling stability at 0.2C and rate performance of EG-LFP. (d-f) Charge-discharge curve, cycling stability at 0.2C and rate performance of EG-LFP.

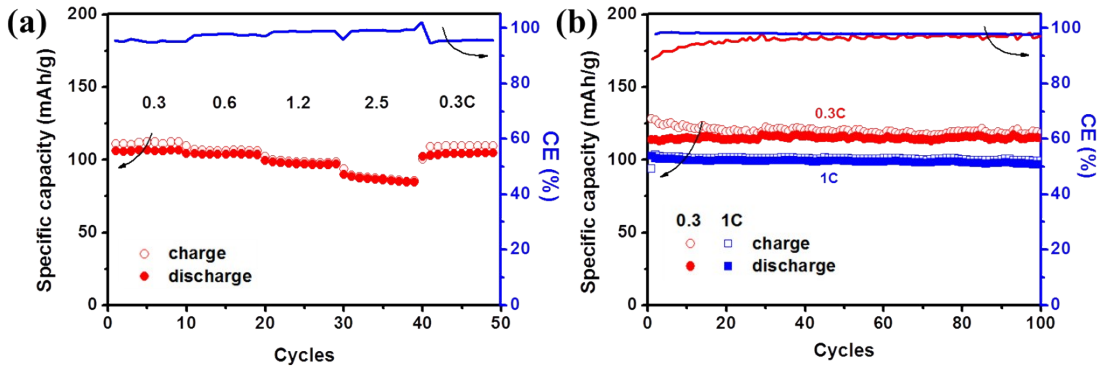

Figure S13. Electrochemical performance of full cells composed of EG-LMO and EG-LTO. (a) Rate capability and (b) cycling performance at 0.3 C and 1 C.

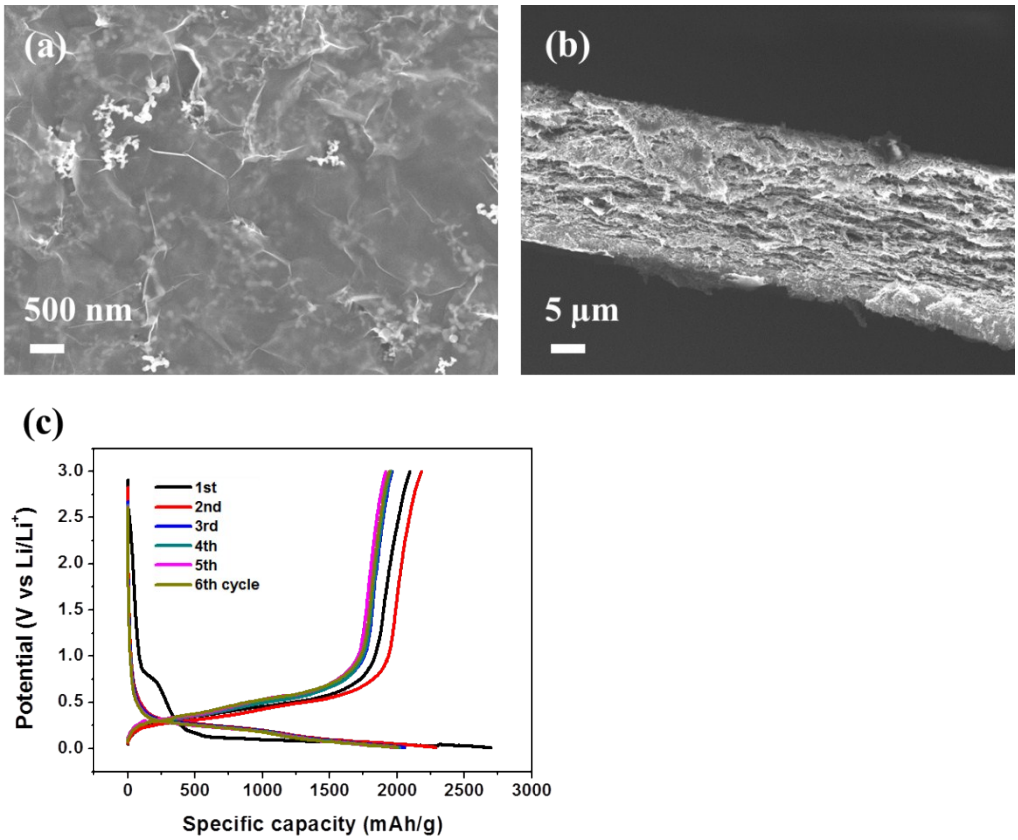

Figure S14. SEM images (a, b) and charge-discharge curves (c) of EG-Si hybrid film. Our co-assembly approach can be used to prepare EG-Si hybrid with Si content of 60 wt%. The resultant EG-Si hybrid shows a similar layer-interlocked structure with Si nanoparticles well confined between EG layers (Figure S14a-b). The electrochemical performance of EG-Si was initially investigated in half cells with Li as anode and commercial 1M $LiPF_6$ in EC/DMC as electrolyte. The potential range is 0.01-3 V vs Li/Li^+. The EG-Si was first activated at 100 mA/g for two cycles and then cycled at 200 mA/g. Due to the limited time for manuscript revision, here we collected electrochemical performance of EG-Si at the first 6 cycles (Figure S14c). At the first cycle, EG-Si showed a high discharge/charge capacity of 2698/2096 mAh/g, corresponding to a Coulombic efficiency of 78%. The irreversible capacity can be assigned to SEI formation. Then the capacity stabilized at 2005 mAh/g. Considering the content of Si (60 wt%) in EG-Si, the Si contributed to a high capacity of 3342 mAh/g, which is slightly lower than its theoretical capacity (3579 mAh/g) and suggests high Si utilization in the EG-Si hybrid.

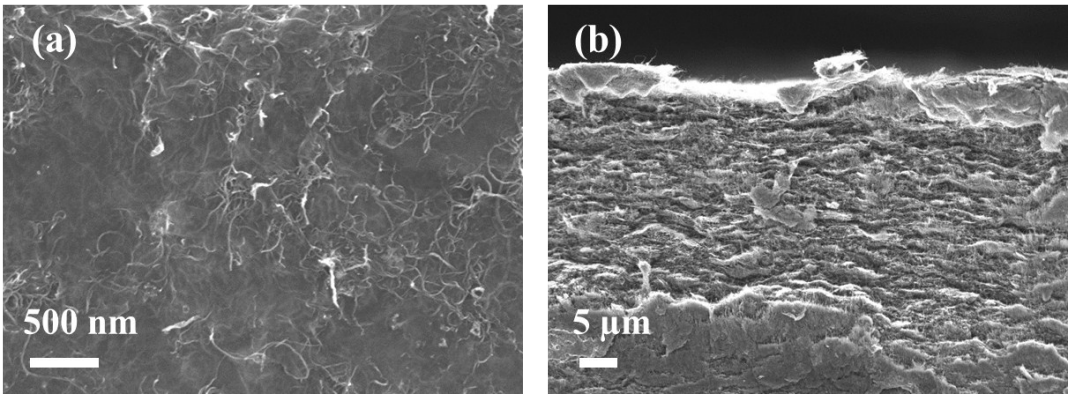

Figure S15. Top-view (a) and edge-view (b) SEM images of EG-CNT hybrid film from.